Optoelectronic and Semiconducting Properties of Conjugated Polymers Composed of Thiazolo[5,4-*d*]thiazole and Arene Imides Linked by Ethynylene Bridges

Mónica Moral,[*,a,c] *Andrés Garzón,*[b] *Jesús Canales-Vázquez,*[a] *and Juan C. Sancho-García.*[c]

* Corresponding author: monicamoralm@gmail.com

[a] *Renewable Energy Research Institute, University of Castilla-La Mancha. Paseo de la Investigación 1, 02071, Albacete, Spain.*

[b] *Department of Physical Chemistry, Faculty of Pharmacy, University of Castilla-La Mancha. Paseo de los Estudiantes, 02071, Albacete, Spain.*

[c] *Department of Physical Chemistry, University of Alicante, 03080, Alicante, Spain*

ABSTRACT

A set of engineered crystalline polymers containing thiazolo[5,4-*d*]thiazole and arene imides linked by ethynylene bridges have been modelled by means of Density Functional Theory (periodic boundary) calculations. A large set of relevant electronic properties related to the opto-electronic and semiconductor character of these systems, such as optical band gap, frontier molecular orbital energy levels, electron affinity, ionization potential, reorganization energy, and electronic coupling between neighboring polymer chains were obtained. We further discuss the effect of the ethynylene linkages, the presence of heteroatoms in thiazolo[5,4-*d*]thiazole rings, and the number of fused rings in the repeating unit on the electronic properties, for disclosing useful structure-property relationship.

INTRODUCTION

New electronic materials are under development for their use in (now conventional) applications, for large-area electronics such as field-effect transistors and photovoltaic cells as well as newly emerged applications, namely integrated sensors, medical imaging arrays, printed radio frequency identification devices, and light-emissive flexible displays, among others, all of them requiring both *p*- and *n*-type components.[1-3] The performance of organic-based devices does not necessarily exceed the level of performance of inorganic semiconductor technologies, though organic materials allow the production of cost-effective, large-area and mechanically flexible electronic devices via solution-based high-throughput patterning techniques.[2,3] The use of organic semiconductors in organic light-emitting diodes (OLEDs), organic solar cells (OSCs), organic thin-film transistors (OTFTs), which in turn can be used for medical and chemical sensing, and organic electrochromic devices as smart-windows and electrochromic mirrors currently attracts a great interest worldwide.[1-4] The organic materials employed in electronic devices are generally divided into two groups: small molecules (or oligomers) and polymers, which shows different advantages or disadvantages in terms of processability and device performance. In general, higher mobilities have been reported for electronic devices fabricated with semiconductors of moderate size than for those fabricated with polymers. Nevertheless, scaling up these results into a reliable and large-area manufacturing process has proven challenging. The typically low viscosity of small molecule formulations may limit the device processing. In addition, the anisotropy of the electronic mobility and mobility loss at the grain boundaries, could alter the optimal performance from device to device, which cannot be tolerated in certain electronic applications.[1]

In this framework, we have chosen, poly(aryl-ethynylene)s (PAEs) polymers that exhibit promising semiconducting and optoelectronic properties, especially when

containing electron-donating and electron-accepting heterocycles linked by ethynylene bridges (-C≡C-).[5-8] Different research groups have investigated the use of PAEs and hyperbranched PAEs as molecular wires, OLEDs, OSCs, OTFTs and fluorescent chemical sensors.[9-14] The interesting electronic properties exhibited by PAEs can be related to the axial symmetry of ethynylene groups, which allows to maintain the conjugation (note that between adjacent aryl groups at different relative orientations rotational barriers are as small as 1 kcal mol^{-1} in these cases)[15-20] across the whole molecular backbone.

In 2005, Yamamoto and co-workers reported the preparation of an electrochemically active PAE including 1,3,5-thiadiazole (Th) as electron-accepting heterocycle.[5,6] During the last years, we have investigated the molecular structure and electronic properties of series of PAEs containing Th as electron-accepting group linked to phenylene and -C≡C- bridges by means of Density Functional Theory (DFT) calculations.[19-23] Their interesting electronic properties make them suitable candidates for their use as organic semiconductors. Going one step further, thiazolo[5,4-*d*]thiazole (TTh) is also an electron-deficient molecule, chemically related to Th, which has been used in the formulation of electrochemically active oligomers and polymers.[24-28] Nevertheless, to the best of our knowledge, no PAEs containing TTh units have been synthesized. Arene imides have also a strong electron-withdrawing character, which lowers the unoccupied frontier orbital and thus might facilitates the charge (electron) injection and concomitant stabilization of the injected charges (electrons). Moreover, the existing π-conjugation is advantageous for intramolecular charge transport[2] and can induce long-distance electronic coupling.[29-30] All these arene imides have already been employed successfully in the fabrication of semiconductor polymers.[2,31] Therefore, a thorough and comprehensive theoretical study of the molecular structure and electronic

properties of a set of PAEs containing TTh and arene imides such as phtalaimide, pyromellitic diimide (PMDI), naphthalene diimide (NDI) or perylene diimide (PDI), connected by -C≡C- bridges (see Chart 1), becomes the goal of the present work. These polymers can be clasified in two main groups: i.e. polymers with linkages to the core instead of the imide position (polymers **II** – **IV**, see chart 1) and polymers with C-N linkages in the backbone (polymers **V** and **VI**, see chart 1). The obtained results will be compared with the parent polymer **I**, without imine groups, and their electronic properties will also be compared with those reported for reference polymers **VII** and **VIII**, in which TTh is substituted by Th and thieno[3,2-b]thiophene (TT) rings.[19-23,32,33]

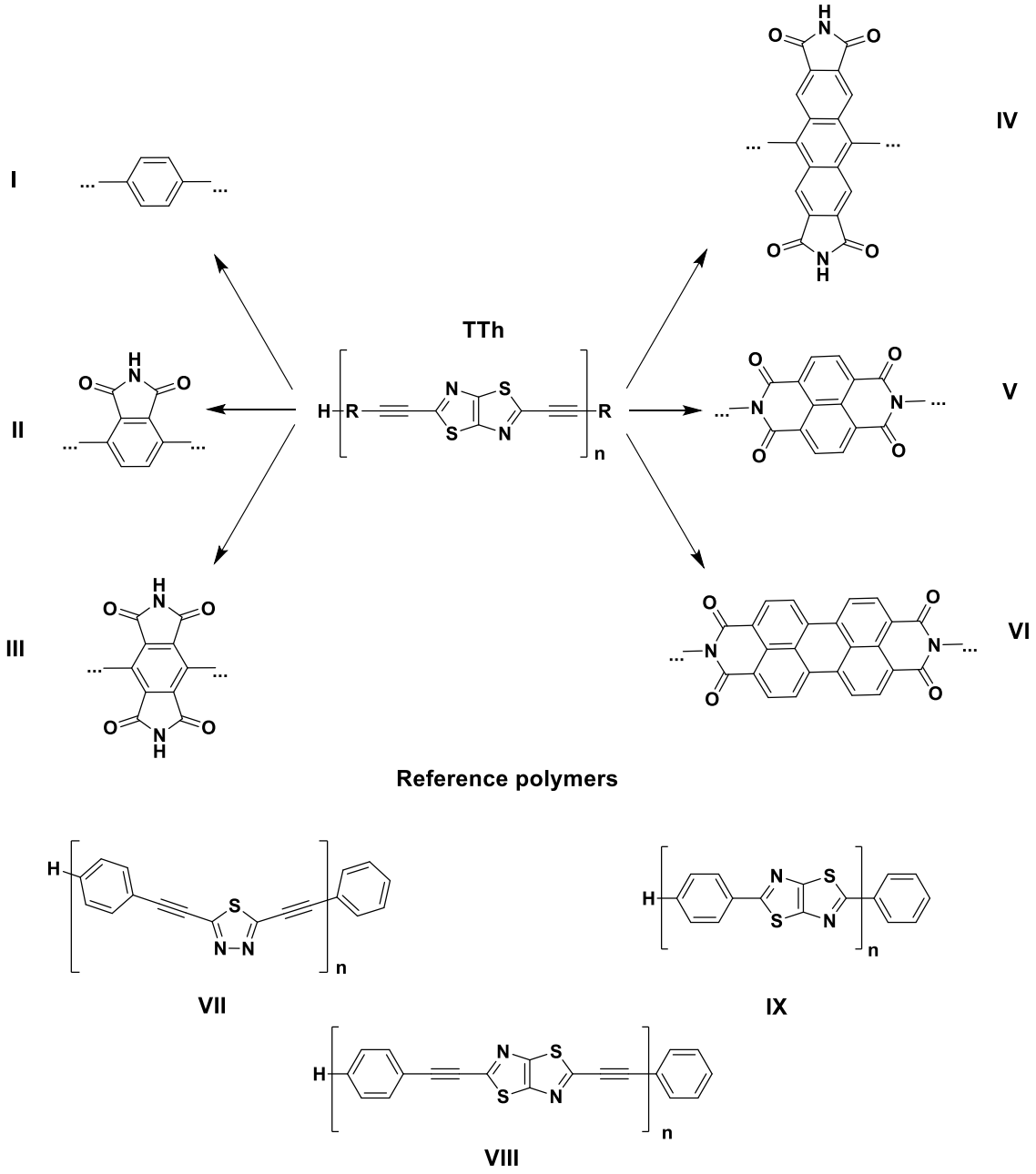

Chart 1. Chemical structures of the studied polymers (**I-VI**) and some related compounds (**VII-IX**) for further comparision.

THEORETICAL CONSIDERATIONS ABOUT CHARGE INJECTION AND TRANSPORT

A high performance in optoelectronic devices is mainly related to efficient charge injection from electrodes and associated charge mobilities. In typical π-conjugated organic crystal materials with small bandwidths (< 1eV) and at room temperature, the

charge migration after injection is generally described by a hopping mechanism,[34,35] where the molecular and lattice vibrations in addition to the coupling with the charge carriers (i.e. the molecular packing as well the conformation of a single molecule) controls the transport efficiency.[36]

In the zero-limit, at high temperature and according to Marcus-Levich-Jortner (MLJ) model,[37,38] the hopping mobility can be modeled as a self-exchange charge-transfer (CT) reaction between neighboring molecules, and estimated through the Einstein-Smoluchoswki relation,

$$\mu_{hop} = \frac{eD}{k_B T} \quad (1)$$

where e is the electron charge, D is the charge diffusion coefficient, k_B is Boltzmann's constant and T is the temperature, fixed here at 298 K. In the case of conjugated polymer crystals where the backbone chains are cofacially stacked, the hopping between neighboring chains is especially favored in the stacking direction. Thus, for a one dimensional charge transport, $D = 1/2\ l^2 k_{CT}$, where l is the distance between the molecules involved in the hopping process and k_{CT} is the rate constant for charge transfer. k_{CT} can be conveniently expressed as:

$$k_{CT} = \frac{4\pi^2}{h} t_{12}^2 \sqrt{\frac{1}{4\pi\lambda_s k_B T}} \sum_{n=0}^{\infty} \left[exp\left(-S_{eff}^n\right) \times \frac{S_{eff}^n}{n!} \times exp\left(\frac{-\left(\lambda_s + n\hbar\omega_{eff} + \Delta G^0\right)^2}{4\lambda_s k_B T} \right) \right] \quad (2)$$

where $\Delta G°$ is the Gibbs free energy of the charge-transfer process (equal to zero in the self-exchange process). In the MLJ formalism, a single effective mode with an energy $\hbar\omega_{eff}$, which represents all the intramolecular modes, is treated at the quantum-mechanical level via the effective Huang-Rhys factor $S_{eff} = \lambda_i/\hbar\omega_{eff}$ ($\hbar\omega_{eff}$ was set here equal to 0.2 eV, which is the typical energy of C-C stretching modes).[39-41] On the contrary, the intermolecular modes are treated classically through the λ_s parameter. In organic crystals, the outer reorganization energy is in the order of few tenths of an electronvolt or lower,

contrary to charge transfer in solution wherein the external part dominates.[3,42-45] Different values for λ_s, ranging between 0.01 and 0.2 eV, have been proposed and employed in literature.[46-49] As in previous works, λ_s was fixed at 0.1 eV in order to facilitate the comparison with previous rate constants reported for PAEs.[23]

The inner reorganization energy, λ_i, for the self-exchange reaction consists of two terms corresponding to the geometry relaxation energies going from the neutral-state geometry to the charged-state and *vice versa* (Nelsen four-point method):[50,51]

$$\lambda_1 = E^0(G^*) - E^0(G^0) \quad (3)$$

$$\lambda_2 = E^*(G^0) - E^*(G^*) \quad (4)$$

$$\lambda_i = \lambda_1 + \lambda_2 \quad (5)$$

where $E^0(G^0)$ and $E^*(G^*)$ are the ground-state energies of the neutral and ionic states, respectively, $E^0(G^*)$ is the energy of the neutral molecule at the optimized ionic geometry and $E^*(G^0)$ is the energy of the charged molecule at the optimized neutral geometry.[3,45,52,53] Since the inner reorganization energy controls the charge-phonon coupling, if $\lambda_1 \approx \lambda_2$, we can write $\lambda_i \approx 2\lambda_1$, and this condition can be satisfied when the molecular structure is not largely deformed during the ionization process.[54]

The charge hopping transport is favored by a small polaron binding energy (E_{pol}), defined as the relaxation energy of an ionized molecule. Taking this into account, both E_{pol} and λ_i must be lowered, while the charge transfer integral, t_{12}, must be maximized in order to improve the charge transport.[36] The charge transfer integral, t_{12}, describes the electronic coupling between two neighboring molecules,[3,44] hence it critically depends on the relative spatial arrangement and is given by the matrix element $t_{12} = \langle\psi_1|\hat{H}|\psi_2\rangle$, where $\hat{H}$ is the electronic Hamiltonian of the system, which in the frame of DFT can be identified with the Kohn-Sham operator. The wave-functions of the initial, ψ_1, and final, ψ_2, charge-localized states are obtained in the hypothetical absence of any coupling between the

molecular units.[23,34,52] Within the framework of the Marcus-Hush two-state model, it is possible to apply the approximate method of the 'energy splitting in dimer (ESD)' in the case of systems with identical and symmetrically equivalent molecules such as ideal polymers.[3,34,52] Strictly speaking, this method requires the use of the geometry of the charged dimer at the transition state. In practice, this process is simplified considering the geometry of the neutral dimer built of two stacked chains with the same conformation as that in the crystal. Then, on the basis of Koopmans' theorem, t_{12}^{-} and t_{12}^{+} (electron and hole transport, respectively) can be obtained by the following equation:

$$t_{12}^{-} = \frac{1}{2}\sqrt{(E_{L+1} - E_L)^2 - (e_2 - e_1)^2} \quad (6)$$

$$t_{12}^{+} = \frac{1}{2}\sqrt{(E_H - E_{H-1})^2 - (e_2 - e_1)^2} \quad (7)$$

where E_{L+1}, E_L, E_H and E_{H-1} are the energies of the LU (Low Unoccupied) MO (Molecular Orbital)+1, LUMO, HO (High Occupied) MO and HOMO–1 levels taken from the closed-shell configuration of the neutral state of the dimer; e_1 and e_2 are the site energies of each isolated molecule in the dimer.[34,35,52] In the case of symmetrically arranged polymers, $e_1 = e_2$ as the infinite chains can be considered as equivalent molecules in the crystal and equation (6) and (7) can be written as.[3,34,45,52]

$$|t_{12}^{-}| = \frac{E_{L+1} - E_L}{2} \quad (8)$$

$$|t_{12}^{+}| = \frac{E_H - E_{H-1}}{2} \quad (9)$$

In that sense, once λ y t_{12} are calculated, absolute k_{CT} and μ values in the stacking direction can be estimated. Both magnitudes are strongly dependent of the morphology of the material. Thus, Marcus hopping model has been successfully applied to reproduce the experimental hole mobilities reported for organic crystals with long-range structural order which are substantially deveid of the influences from thermal and energetic disorder.[55] On the contrary, the best reproduction of the experimental mobilities in thin

film materials has been obtained considering thermal and energetic disorder. The presence of grain boundaries between crystalline domains is a source of disorder in these materials and hinder the charge transport.[55] In the present study, we have worked under the assumption of perfect crystalline polymer and, hence, the calculated mobility for each polymer corresponds to a maximum limit value. Relative hopping mobilities, μ_{rel}, were also calculated for comparative purposes since those can be more informative and reliable than the absolute values considering the assumed approximations in our model.[53]

To achieve a good charge injection, the frontier MOs and the work-function (Φ) of the electrode must have appropriate values. An ohmic contact is produced when the difference energy between the frontier MO and Φ is equal or lower than 0.3 eV. In the case of *p*-type semiconductors, the HOMO must be aligned with the Fermi levels of environmentally stable anodes, such as ITO[56] to obtain an efficient hole injection. By contrast, in the case of *n*-type semiconductors, the LUMO should match the Fermi level of the electrodes, with low work function, such as Ca, Mg, Ba or Al.[57] Although this is an approximation, i.e. interface dipole effects between the electrode and semiconductor have not been taken into account,[46,58] the comparison of Φ with HOMO/LUMO energy levels of the semiconductor may help to determine whether charge injection is likely or, on the contrary, high contact resistance should be expected. Moreover, the values of the HOMO and LUMO orbitals must range between -4.8 – -5.5 eV and -3.6 – -4.5 eV, respectively, to improve the stability of the opto-electronic device.[3] However, some studies establish the limiting value for LUMO energy in -4.0 eV, as the negative charges can react with atmospheric oxidants such as water or oxygen.[59,60]

Ionization potential (IP) and electron affinity (EA) are also key parameters that determine the efficiency of the charge injection from the electrodes in addition to the susceptibility to be reduced or oxidised upon air exposure.[53] Thus, the EA of a

semiconductor must be ≥ 3.0 eV for an easy electron injection, but not much greater than 4.0 eV to avoid destabilization under ambient conditions.[42] Low IPs facilitate hole injection, though too low values may produce unintentional doping.

COMPUTATIONAL DETAILS

The Gaussian09 (Rev. D.01) package has been employed for all the calculations reported here.[61] Different DFT hybrid functionals were employed, i.e. B3LYP,[62,63] PBE0,[64] and M06-2X,[65] along with the 6-31G* basis sets, for the computation of the electronic properties of the studied PAEs. The choice of different hybrid (B3LYP, PBE0 and M06-2X) functionals allowed us to study the influence of the variable fraction of the exact-like exchange in the functional, i.e. 20% for B3LYP, 25% for PBE0, and 52% for M06-2X, on some of the studied properties.

The optical band gap was estimated through electronic transitions with high oscillator strength values ($f \geq 1.0$) involving frontier MOs extended along the whole system, (generally HOMO → LUMO transition except for oligomers **V** and **VI**). The energy of the transition was obtained by the time dependent (TD)-DFT formalism,[66] using again the B3LYP, M06-2X and PBE0 hybrid functionals together with the 6-31G* basis set, on oligomeric structures from 1 to 15 repeat units (n), excluding some oligomer chains because of the large demand of computational resources. Note that oligomers with different chain length ($n = 3 - 15$) were generated by replication of the minimal periodic motif, which was previously optimized at the same level of theory and in those cases the free valences were saturated with hydrogen atoms.[21,23,32,67-69] We have observed that this procedure allows calculating electronic properties in long oligomeric chains with a great reduction of the computational cost, and without significantly affecting the optical band

gap.[21] The values of the optical band gap for the ideal polymer chains were estimated through the equation proposed by Meier *et al*.[70]

$$E(n) = E_\infty + (E_1 - E_\infty) \exp[-a(n-1)], \quad (10)$$

where E_1 and E_∞ stand for the excitation energies for the monomer and the infinitely long polymer, respectively; n is the number of repeat units and a is an empirical parameter that describes how fast $E(n)$ saturates to E_∞.

The HOMO/LUMO energy value (E_{HOMO}/E_{LUMO}), IP/EA and λ_i were calculated at the B3LYP/6-31G* level on previously optimized oligomers at the same theory level. The chain length of the modelled oligomers was increased up to saturation of the monitored properties ($n \leq 13$). Closed-shell calculations for singlets and open-shell calculations for doublets (cationic and anionic species) have been carried out for the different oligomer chains. To perform those calculations, B3LYP was the method of choice, as it yields reasonable conjugated-polymer ground-state structures[33,71-73] and, in general, seems appropriate for the prediction of electronic structures of polycyclic aromatic hydrocarbons.[29,74] In addition, that method usually provides theoretical λ_i values in good quantitative agreement with the corresponding experimental gas-phase ultraviolet photoelectron spectroscopy estimates,[75] togheter with satisfactory linear relationships between calculated E_{HOMO}/E_{LUMO} and experimental IPs/EAs in such a way that the calculated E_{HOMO}/E_{LUMO} can be used to semi-quantitatively estimate EAs/IPs[76-78] and orbital energies.[79] Although Koopmans' theorem is not strictly applicable to Kohn-Sham orbital energies,[80] Janak's theorem proved a connection between IP/EA and E_{HOMO}/E_{LUMO} (see ref [78] and references therein). The values of E_{HOMO}/E_{LUMO}, IP/EA and λ_i for the infinitely long polymer chains were estimated through a single exponential function similar to that proposed by Meier *et al.* for the band gap.[70]

The crystal structures were modelled at the HSE06/6-31G* level [81-83] by means of periodic calculations using a single repeating chain. The spatial arrangements of two stacked periodic chains, exhibiting minimum binding energy (E_{bind}), were used as starting point for the crystal structure modelling. With that goal in mind, E_{bind} landscapes were calculated for two periodic chains which were kept with face-to-face planes at a distance of 3.5 Å along *z*-direction, corresponding to a typical π-stacking distance (see Figure 1). While the position of one of the chains was kept fixed, the second chain was displaced along *x*- and *y*-axes in a grid of 1.0 Å in both directions. HSE06 has been purposefully chosen for the crystal structure modelling, thanks to the use of a screened Coulomb potential by splitting the corresponding two-particle operator into a short-range (SR) and a long-range (LR) terms, which is highly recommended for calculations of band gaps and lattice constants in solids.[81-83] Although HSE06 was originally developed for inorganic semiconductors, the combination of a screened hybrid functional with empirical dispersion correction terms has also been proven adequate for modelling π-conjugated polymers.[22]

Once the crystal structure was obtained, t_{12} values between neighboring chains were calculated at the B3LYP/6-31G* level for each studied polymer. These t_{12} values were obtained from the band structure of two stacked, isolated chains at the Γ point as half the energy splitting of the HO and LU Crystal Orbital (CO) levels.[34,53] Similar to the E_{bind} landscapes, t_{12} values were also scanned as a function of the *x*- and *y*-axes displacement of a polymer chain keeping fixed z = 3.5 Å (a typical π-stacking distance) an identical chain. The 6-31G* basis set was chosen because it provides a reasonable trade-off in periodic boundary calculations between accuracy and computational cost. Nevertheless, several investigations have previously reported that the use of other basis

sets such as 6-31G*, 6-31+G*, and 6-311G** does not produce significant differences in the calculated t_{12} value.[4,35]

RESULTS AND DISCUSSION

Polymer crystal structure. As stated before, the crystal structures of the polymers were modelled using as starting point the spatial arrangements of two stacked periodic chains where their binding energy displays the lowest value. Figure 1 shows the energy landscapes obtained for dimers formed by the polymer chains **I** – **VI**, as a function of the relative *x*,*y*-displacement of one chain with respect to the other. The lowest-energy (*x*,*y*) coordinates calculated for all the studied polymers are collected in Table 1. The optimized unit cell parameters are also shown in Table 1. All the calculated polymer chains remained highly planar, showing values $\leq 0.1^{o}$ for the dihedral angle, $|\tau|$, which describes the torsion between a TTh ring and the next aromatic ring in the chain. That contrasts with the dihedral angles between neighboring aryl groups of up to 18.5^{o} observed for the reference polymer **VII**.[22] A plane that contains approximately all the TTh rings of a same chain can be defined and *1* (see Table 1 and Figure 2) corresponds to the distance between that plane and its parallel neighboring plane (stacking distance). A distance between planes of 3.5 Å was calculated for all the polymer crystal structures except for the polymers **I** (3.8 Å) and **IV** (3.3 Å). Therefore, it seems that the presence of imide groups in the set of the polymers studied leads to shorter stacking distances. For the polymers containing imide groups (**II** – **VI**), no clear correlation between the number of fused aromatic rings of the repeating unit and the stacking distance was observed.

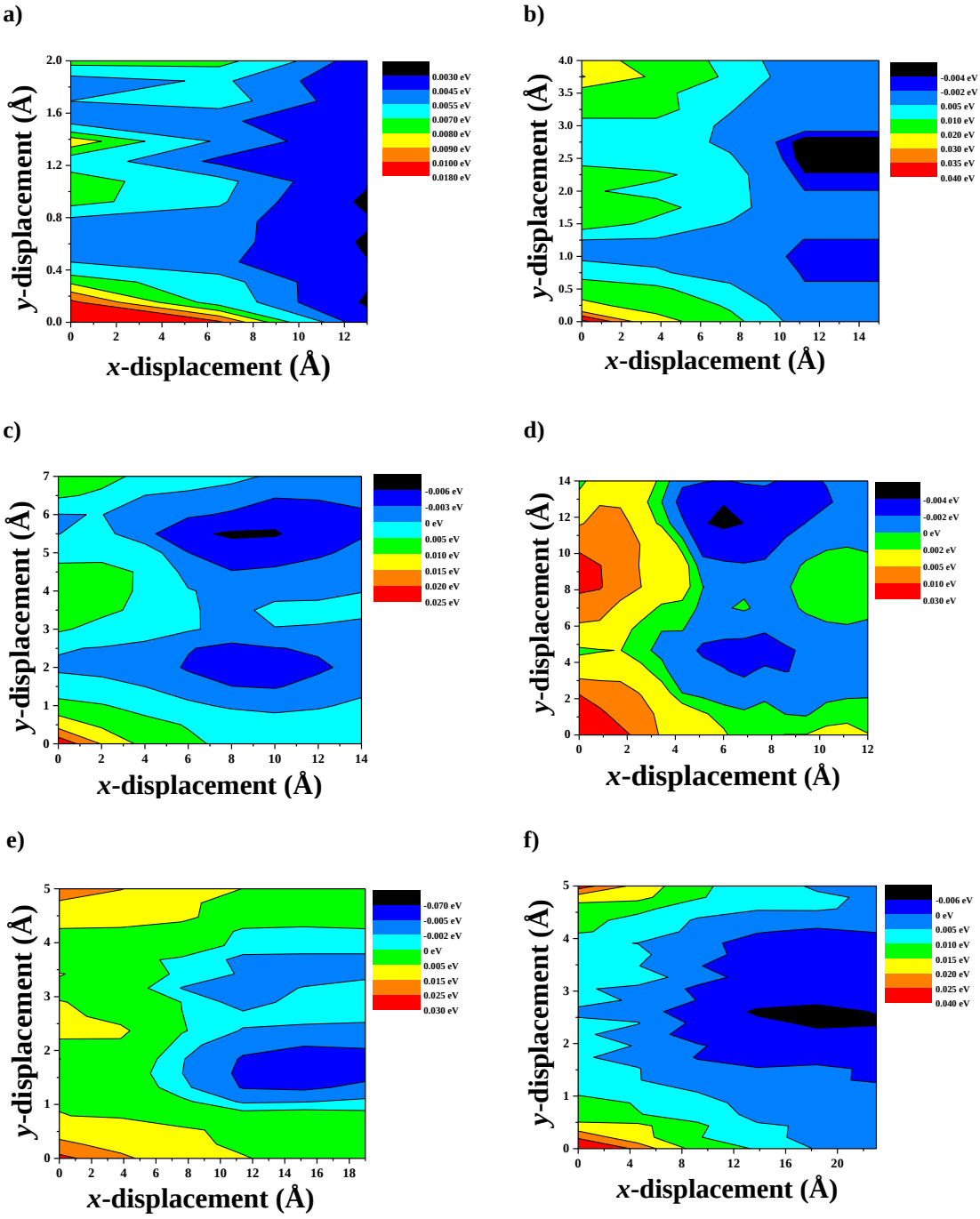

Figure 1. Binding energy landscapes calculated for dimers formed by the polymer chains I – VI as a function of the relative (x,y)-displacement of one chain, in a plane, with respect to the next, in a parallel plane. The z-displacement was kept fixed z = 3.5 Å. (a) Corresponds to polymer I; (b) to II; (c) to III; (d) to IV; (e) to V and (f) to VI.

Table 1. Relative *x,y*-displacements corresponding to the minimum E_{bind} values calculated at the B3LYP/6-31G* level for dimers formed by two polymer chains. Optimized unit cell parameters calculated at HSE06/6-31G* level along with the dihedral angle, |τ|, between a TTh ring and the next aromatic ring in the polymer chain and the stacking disntace, *l*, between two parallel planes containing neighboring polymer chains.

Polymer	Dimers	Crystal polymer structure							
	x,y-displ. (Å)	Cell lengths (Å)			Cell angles (º)			*l* (Å)	|τ| (º)
		a	b	c	α	β	γ		
I	6, 2	15.27	11.85	5.02	50.48	49.36	29.71	3.8	0.00
II	11, 3	30.60	13.56	5.17	69.70	45.97	46.75	3.5	0.00
III	11, 4	15.31	13.56	5.15	66.47	45.50	44.18	3.5	0.00
IV	9, 7	15.27	16.39	5.10	58.00	45.48	68.67	3.3	0.00
V	6, 4	19.34	12.86	8.65	83.08	29.81	57.84	3.5	0.10
VI	12, 4	23.63	12.46	14.10	56.48	22.27	38.20	3.5	0.00

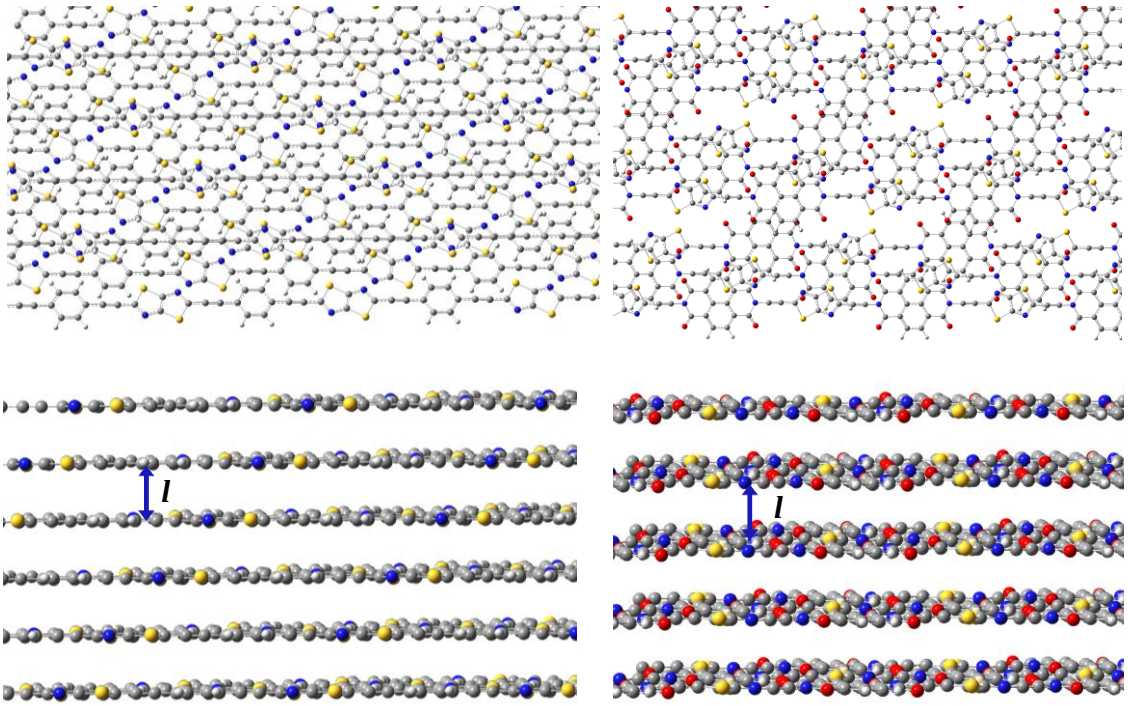

Figure 2. Different type of arrangements of polymer **I**, on the left, and polymer **V**, on the right. *l* corresponds to the stacking disntace.

Optoelectronic properties. The optical band gap is a key property related to the performance of polymer solar cells. In general, the photocurrent in these devices is limited by the overlap between the absorption spectrum of the polymer and the solar spectrum,

which reaches the maximum photon flux around 1.6 – 1.8 eV.[84] Table 2 shows the optical band gap values estimated for the infinite polymer chains through the equation (10) except for the **V** and **VI**, for which the corresponding values calculated for the oligomers $n = 5$ are shown (more detailed information on the oscillator strength, main components of the transitions and values obtained in the different fits are collected in the Supporting information, Tables 1S – 6S). As previously mentioned, different TD-DFT levels were employed for the calculations and those with the highest percentage of exact-like exchange yielded the highest optical band gap values.[32,33,68,69] The shapes of the frontier MOs of monomers **I**, **IV**, **V** and **VI** and their oligomers with n = 5 are shown in Figure 3. In general, HOMO and LUMO are π and π* MOs delocalized over the whole molecule or polymer chain. Similar observations have been previously reported for other PAEs.[23,32,69] However, in the case of the polymers involving C-N linkages in the backbone (**V** and **VI**), HOMO, LUMO and a large number of frontier MOs are localized over certain TTh and arene imide units. In fact, the optical band gap could not be determined for long oligomers **V** and **VI** due to the large demand on computational resources needed to calculate the first electronic transition with high f and involving frontier MOs extended along the whole oligomer chain.

Table 2. Calculated optical band gaps for the studied oligomers and values estimated for the corresponding infinite polymer chains.

Polymer	*n*	Band gap (eV)		
		TD-B3LYP/6-31G*	TD-M06-2X/6-31G*	TD-PBE0/6-31G*
I	n→∞[a]	2.062 ± 0.034	2.907 ± 0.006	2.232 ± 0.014
II	n→∞[a]	1.994 ± 0.012	2.822 ± 0.010	2.154 ± 0.012
III	n→∞[a]	1.855 ± 0.012	2.668 ± 0.010	2.011 ± 0.012
IV	n→∞[a]	1.431 ± 0.012	1.990 ± 0.012	1.573 ± 0.012
V	5	2.696	3.541	2.905
VI	5	2.314	2.766	2.407

[a] Values for infinite polymer chains were estimated from a fit to the equation (10).[70]

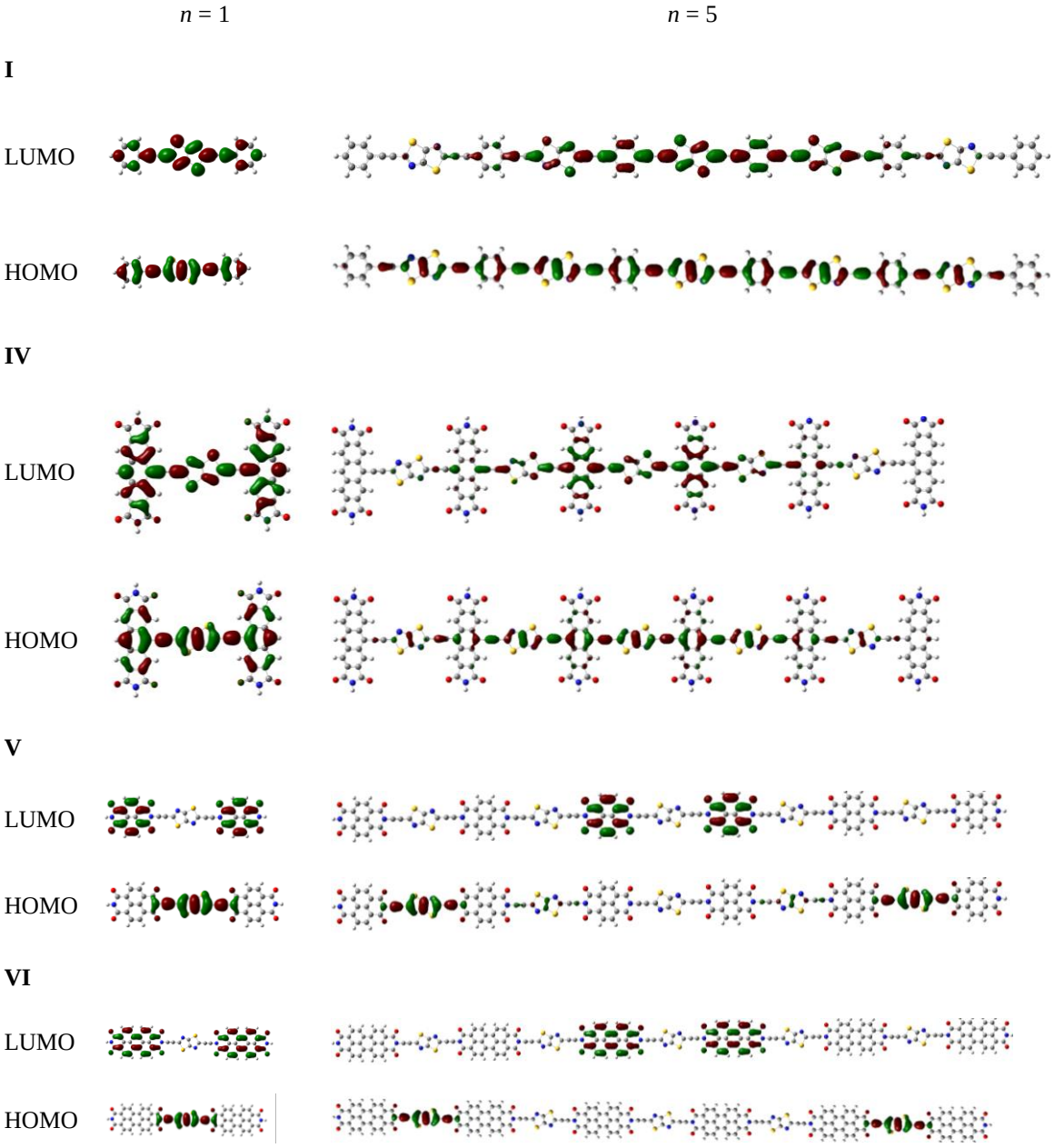

Figure 3. Isocontour plots (0.02 a.u.) of frontier molecular orbital calculated for **I**, **IV**, **V** and **VI** polymers with *n* = 1 and 5 at the B3LYP/6-31G* level.

Taken as a representative example, Figure 4 illustrates the optical band gap dependence with the chain length along the corresponding fitting to equation (10) for the polymers **I** – **IV** (see also Figure 1S and 2S of the Supporting Information). As can be

easily seen, oligomers with n = 15 are long enough to ensure the saturation of the band gap value and a suitable fitting to equation (10) ($r^2 > 0.998$, in all cases) (more detailed information about the values obtained in the different fits can be found in Table 7S of the Supporting information). In all cases, the band gap tends to decrease with increasing the chain length, reaching a saturation value at $n \geq 11$. The number of fused aromatic rings has a clear effect on the reduction of the band gap in oligomers **I** – **IV**. In the field of photoactive materials, only the calculated band gaps for the oligomers **IV** with $n \geq 3$ (at the TD-B3LYP and TD-PBE0 levels) and the corresponding estimated values for the infinite chains satisfy the needed condition of overlap with the maximum absorption of the solar spectrum. As a consequence, these oligomers could be promising candidates for the fabrication of solar cells. The band gaps calculated for long oligomers **III** ($n \geq 9$) (at the TD-B3LYP level) also lie near the threshold of 1.8 eV,[84] with similar values to the pryomellitic diimide (PDMI) analogues reported by Guo and Watson.[85] Regarding polymers **V** and **VI**, the band gap values are similar to their PDI or NDI single monomers.[86] Observing these values, they could indicate that the imide rings ultimately control the band gap values.

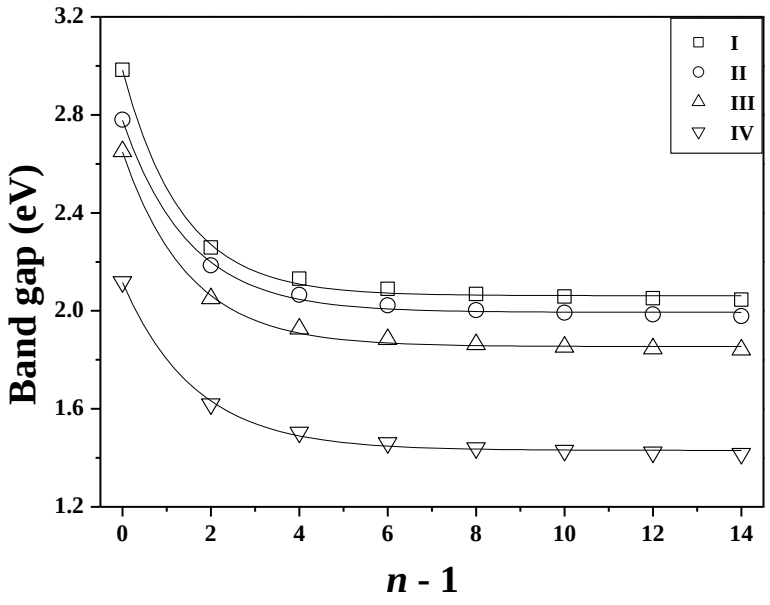

Figure 4. Optical band gap values calculated for oligomers **I** – **IV** with different chain lengths at the TD-B3LYP/6-31G* level and fits to the equation proposed by Meier et al.[70]; (□) correspond to oligomers **I**; (○) to **II**; (Δ) to **III**; and (∇) to **IV**.

Previously, we reported an optical band gap of 2.371 ± 0.029 and 2.07 eV (calculated at the TD-B3LYP/6-31G* level) for the infinite polymer chains **VII** and **VIII**, respectively. The value estimated for the infinite chain **I** is ~ 0.3 eV lower than that reported for **VII** and similar to the corresponding value of **VIII**. Here, we observe again that the number of fused aromatic rings lowers the band gap. As far as we know, the studied polymers have not been synthesized yet, but the synthesis of some related compounds to **I** such as the monomer and oligomer **IX** has recently been reported.[87,88] For the monomer **IX**, a HOMO → LUMO transition energy ~ 0.6 eV higher than the corresponding energy obtained for the monomer **I** was calculated (at the same level of theory).[87] Therefore, the introduction of ethynylene moieties, along with the increase of the number of fused rings in the repeating unit, seems to be a suited strategy to reduce the optical band gap of these PAEs.

Charge transport properties. The calculated λ_i values for both electron and hole injection decrease with lengthening of the polymer chains (see Figure 5, Table 3 and Table 8S – 9S of the Supporting Information). For small conjugated oligomers, the charge carrier - phonon assembly (so-called *polaron*) can delocalize over the whole molecule and, hence, λ_i strongly depends on the size of the oligomer. Figure 6 shows the delocalization of the α-SOMOs (Single Occupied Molecular Orbitals) of the ion oligomers **I** and **IV**. Nevertheless, α-SOMOs of the ion oligomers containing C-N linkages in the backbone (**V** and **VI**) are not as delocalized as the rest of the α-SOMO orbitals. When the length of the oligomers steadily increases, λ_i shows an asymptotic behaviour with respect to the oligomer size.[68,71,89] The perturbation of the geometry caused by the presence of a charge becomes almost negligible for long chains and the low

value of λ_i can be associated to largely extended and weakly bound polarons.[45] Note that extreme polaron delocalization associated to a very low reorganization energy has been recently measured for π-conjugated porphyrin oligomers.[90]

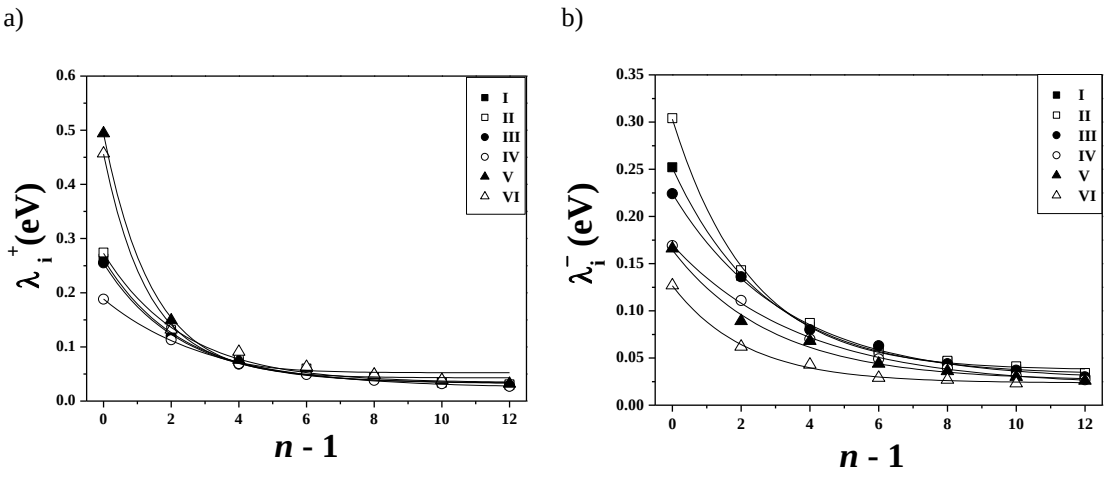

Figure 5. Calculated (a) λ_i^+ and (b) λ_i^- for oligomers of different chain length at the B3LYP/6-31G* level and fitted to the equation proposed by Meier et al.[70]

Polymer $I_{n=5}$

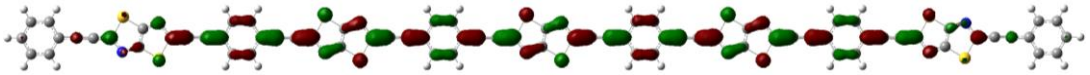

α-SOMO anion

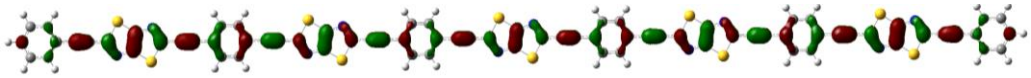

α-SOMO cation

Polymer $IV_{n=5}$

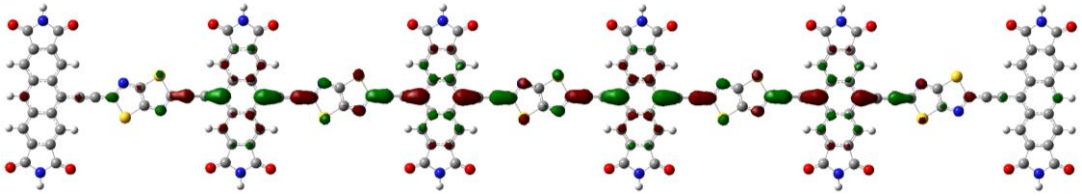

α-SOMO anion

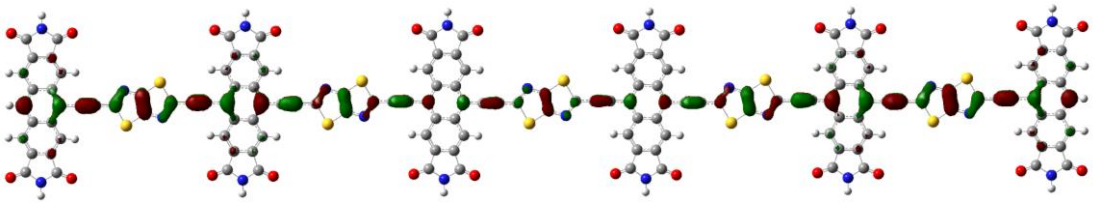

α-SOMO cation

Polymer $V_{n=5}$

α-SOMO anion

α-SOMO cation

Figure 6. Isocontour plots (0.02 a.u.) of α-SOMOs, for cations and anions, calculated for different anionic oligomers at the B3LYP/6-31G* level.

As described before, a single exponential equation analogous to equation (10) was employed to fit the λ_i values as a function of *n* and to obtain an estimate at the polymer limit (see Figure 5). These estimated λ_i values for the infinite polymer chains are within the 0.020 – 0.037 eV and 0.024 – 0.054 eV ranges for electron and hole transport, respectively. The data are collected in Table 3 ($r^2 \geq 0.993$ in all fits, see Table 10S – 11S in the Supplementary Information) and show, in general, how internal reorganization energies estimated for electron transfer (λ_i^-) in the infinite polymer chains are close to those calculated for hole transfer (λ_i^+). Nevertheless, λ_i^- values of about half of λ_i^+ were obtained for the polymers with C-N linkages in the backbone. The lowest λ_i^- values were estimated for the polymers with more fused rings in arene imide units, i.e. polymers **IV** (0.020 ± 0.004 eV) and **VI** (0.023 ± 0.004 eV). λ_i^- values have previously been reported for oligomers analogous to **I** (at the same level of theory) but containing Th and TT rings

instead of TTh.[23,32,33] λ_i^- values estimated for the infinite polymer chain **VII** (0.032 ± 0.006 eV) and calculated for its short oligomers are similar to those obtained for the polymer **I** (0.032 ± 0.002 eV) and the corresponding oligomers.[23] On the other hand, a significant increase in λ_i^- of ~ 0.02 eV is observed for the infinite polymer chain **VIII**, which does not contain nitrogen atoms in the chemical formula.[33] Therefore, the change of Th by TTh does not seem to have an important influence on λ_i^- but the presence of nitrogen atoms allows reaching lower electron reorganization energies for these conjugated polymers. In general, for all the studied systems, low reorganization energies were calculated for short oligomer lengths and even for monomers. For example, the λ_i^- values calculated for the monomers **IV** – **VI** (0.127 – 0.169 eV) and for the oligomers **I** – **III** with n = 3 (0.136 – 0.143 eV) are comparable or lower than those calculated at the B3LYP/6-31G** level for compounds proposed as *n*-type organic semiconductors such as pentacene (0.132 eV),[78] a perylenediimide derivative (0.272 eV),[91] rubrene derivatives (0.098 − 0.127 eV),[92] some coronene-diimide derivatives (0.226 – 0.241 eV),[29] the infinite naphtalene-carboxydiimide polymer chain ($\lambda_i^- \approx 0.2$ eV)[93] and some fluorinated perylene diimides ($\lambda_i^- = 0.27 – 0.35$ eV).[94] In the case of hole transport, the lowest λ_i^+ was also estimated for the polymer **IV** (0.024 ± 0.002 eV) while the highest values were obtained for the polymers with C-N linkages in the backbone such as **V** and **VI** (0.043 ± 0.010 and 0.054 ± 0.016 eV, respectively). λ_i^+ values calculated for the monomer **IV** (0.188 eV) and for the rest of oligomers with n = 3 (0.120 − 0.149 eV) are comparable to those reported for some tetratiofulvenes (TTF) (0.071 − 0.234 eV, calculated at the B3LYP/6-31G** level) (see reference [95] and references therein), oligoacenes and oligothiopenes (0.077 − 0.182 eV, calculated at the B3LYP/6-31G** level)[96] which have been demonstrated to behave as high mobility *p*-type semiconductors in OFETs. Summarising, the lowest reorganization energies for both electron and hole transfer were

calculated for the oligomers of compound **IV**. The reorganization energies estimated for the infitine polymer chains **IV** are at least 25% lower than those obtained for the homologous polymer **III** which containes two less fused rings in the repeat unit. Hence, it seem that the presence of nitrogen atoms in TTh and Th rings, together with higher number of fused rings in the arene imide unit, reduces the perturbation of the geometry caused by the presence of a negative charge. Consequently, low λ_i^- values were also obtained for oligomers of compound **VI**. On the contrary, for hole transfer, the linkage to the core instead of the imide position seems to lower λ_i^+.

Table 3. Predicted Electron Affinity (AEA and AEV), Ionization Potential (AIP and VIP), Reorganization Energy (λ_i^+ and λ_i^-) for an infinite and ideal polymer chains. Calculations were carried out at the B3LYP/6-31G* level.[a]

	Holes			Electrons		
Polymer	AIP (eV)	VIP (eV)	λ_i^+ (eV)	AEA (eV)	VEA (eV)	λ_i^- (eV)
I	5.772±0.040	5.789±0.042	0.033±0.004	2.821±0.060	2.804±0.062	0.032±0.002
II	6.061±0.044	6.084±0.046	0.033±0.006	3.199±0.046	3.177±0.050	0.037±0.004
III	6.234±0.046	6.251±0.048	0.032±0.004	3.516±0.044	3.501±0.046	0.027±0.006
IV	5.971±0.036	5.983±0.036	0.024±0.002	3.777±0.044	3.767±0.044	0.020±0.004
V	6.137±0.032	6.167±0.036	0.043±0.010	3.743±0.034	3.720±0.054	0.026±0.008
VI	5.871±0.042	5.924±0.032	0.054±0.016	3.691±0.018	3.666±0.034	0.023±0.004

[a] Corresponding to the infinite polymers chains; the error corresponds to ±2σ, where σ is the standard deviation with respect to the first order exponential fitting.[70]

The electronic coupling strongly depends on the relative arrangement of the molecules in the crystal, with the main electron-hopping pathway found along the π-stacking direction, whereas the electronic coupling between coplanar chains can be generally considered negligible.[4,22,33] For two perfectly stacked molecules, it is known that small molecular displacements may also lead to significant changes in the t_{12} value.[45] Figure 7 shows indeed strong oscillations in the value of t_{12} for displacements of polymer chains **I** and **V** along the *x*- and *y*-axes in dimers consisting of two π-stacked infinite chains. These characteristic profiles are related to the nodal pattern of the HOMO-1/HOMO and LUMO/LUMO+1 orbitals of the polymer chains being the hole or electron coupling

maximised for the maximum overlap position in most of the cases.[45] Table 4 collects the t_{12} values calculated for dimers of stacked chains, taken from the previously modelled crystal structure in the Γ point of the band structure. Electronic couplings for hole transfer (t_{12}^{+}) are at least 1.8-fold higher than those corresponding to electron transfer (t_{12}^{-}) except for polymer **VI**. The highest values of both t_{12}^{-} and t_{12}^{+} were calculated for the polymer with the smallest predicted cofacial distance between the two neighboring chains (polymer **IV**, l = 3.3 Å), followed by the values obtained for polymers **I** and **II**. On the other hand, low electronic couplings were in general obtained for the polymers containing C-N linkages (**V** and **VI**). Comparable t_{12}^{-} values were calculated for the linear polymer chain **I** and for the zig-zag polymer chain **VII**,[23] which contain TTh and Th units, respectively. Nevertheless, low electronic couplings have been reported for the polymer containing TT rings (**VII**)[33] which suggests that the presence of nitrogen atoms in the electron-accepting unit may improve the semiconducting properties of this kind of polymers. In general, t_{12}^{-} values calculated for polymers **I**, **II** and particularly **IV** lie in the range of those reported for the different pathways within the pentacene crystal (0.043 − 0.084 eV, calculated at B3LYP/6-31G** level from a crystal structure)[97] and for analogous systems, such as oligothiophenes made up of 6 repeat units (0.132 eV, calculated at the B3LYP/6-31G** level) and short oligomers formed by thiophene rings and perfluoro-phenyl units (0.01 – 0.07 eV, calculated at the B3LYP/6-31G** level).[98] In the case of hole transport, t_{12}^{+} values calculated for polymers **I** – **V**, especially for **II** and **IV**, are comparable to the values reported for oligomers such as oligothiophene with n = 6 (0.135 eV, calculated at the B3LYP/6-31G** level), short oligomers formed by thiophene rings and fluoroarenes-thiophenes (0.031 − 0.057 eV, calculated at the B3LYP/6-31G** level),[98] and compounds such as thiophene-pyrrole based oligo-azomethines.[99] It is worthy to be mentioned the strong differences calculated for the

electron couplings of the polymers **III** and **IV** which present related structures. In this case, the higher number of fused rings can be associated to the increase of the coupling between neighboriong rings.

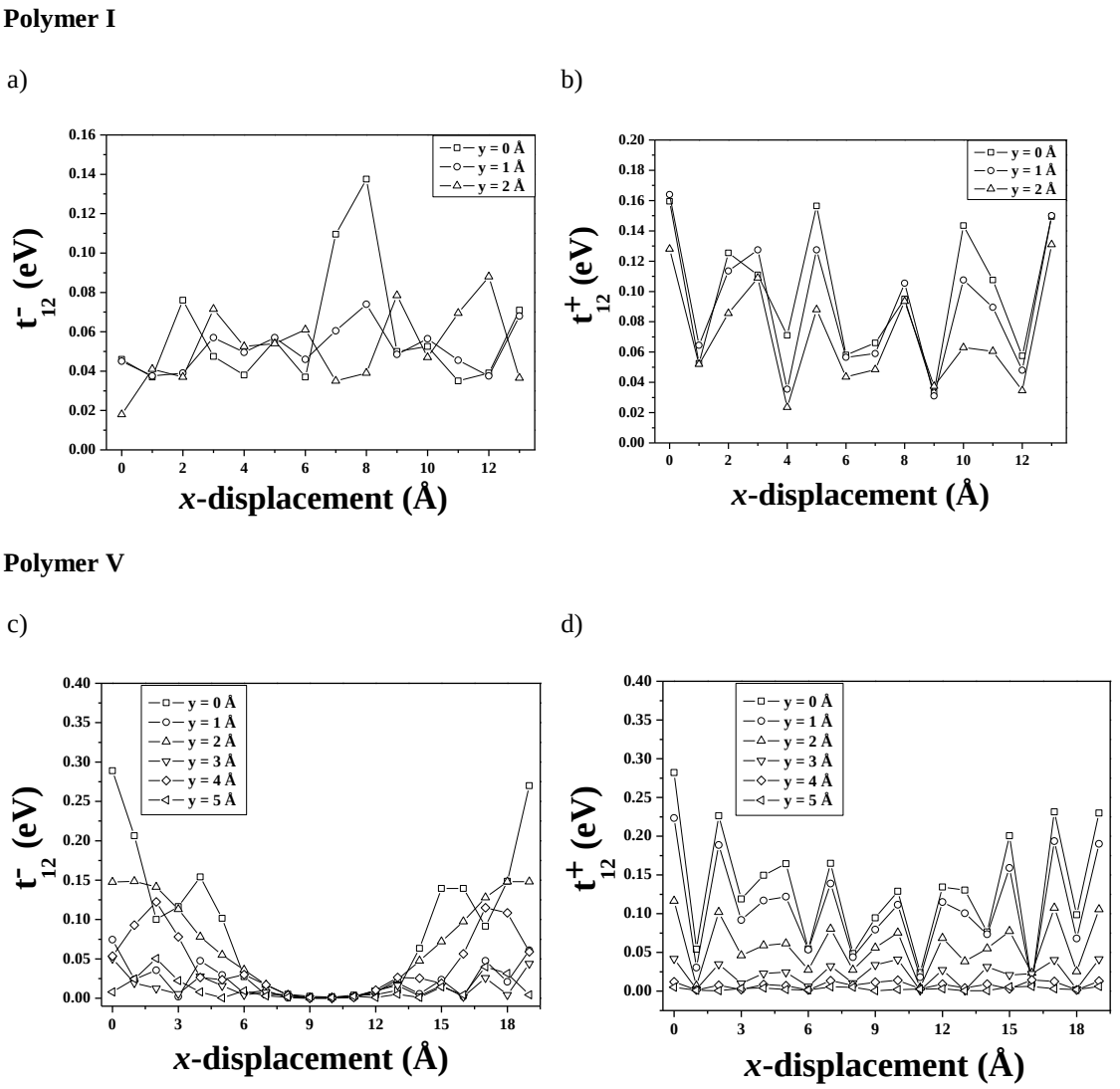

Figure 7. Evolution of calculated t_{12} values as a function of the degree of translation of one chain along the *x*-and *y*-axes in a system consisting of two π-stacked polymer chains (**I** and **V**) with an intermolecular distance fixed at 3.5 Å.

The values estimated for the charge transfer constants along the π-stacking direction and charge mobilities at 298 K are also collected in Table 4. In general, a more

pronounced *p*-type rather than *n*-type character is expected for the studied PAEs since k_{CT}^{+} / k_{CT}^{-} ratios are within 3 – 15 for polymers **I** – **IV**. That ratio is only lower than 1 for polymer **VI.** Both charge transfer rate constants estimated for polymer **I** are higher than the rate constant reported for polymers containing Th and TT units (**VII** and **VIII**).[23,33] Hence, the use of TTh instead of Th and TT could improve the semiconducting properties of these PAEs. The highest rate constants for both electron and hole transport and, therefore, the most efficient charge transport were predicted for polymer **IV**. The lowest k_{CT} values were in general obtained for the polymers with C-N linkages in the backbone (**V** and **VI**).

The relative values of the mobility, μ_{rel}^{+} and μ_{rel}^{-}, with respect to the parent polymer **I**, and the comparison with the values reported for the reference polymers **VII** and **VIII**, might provide valuable information to analyze the effect of the different aromatic units on the semiconducting properties of the studied PAEs. Thus, $\mu_{rel}^{-} > 1$ were only obtained for polymer **IV**, while in the case of hole hopping, $\mu_{rel}^{+} > 1$ was calculated for both polymer **II** and **IV**. Again it must be highlighted the case of polymer **IV**, that shows the highest absolute mobilities for electrons and also for hole transport. Polymer **I** also shows high absolute mobilities, and along with **IV**, relatively balanced μ^{+} and μ^{-} ratios of 0.3 – 0.4. These ratios are similar to those calculated for other ambipolar semiconductors used in opto-electronic devices, where the electron mobility is typically about three times lower than the hole mobility.[100]

Table 4. Electronic couplings (t_{12}^+ and t_{12}^- in eV), charge transfer rate constants (k_{CT}^+ and k_{CT}^- in s^{-1}), absolute and relative hopping mobilities (μ^+ and μ^- in $V^{-1}\ cm^2\ s^{-1}$ along with μ_{rel}^+ and μ_{rel}^-) and μ^-/μ^+ ratio calculated for the series of studied PAEs. Calculations were carried out at the B3LYP/6-31G* level.

Polymer	t_{12}^-	$k_{CT}^- \times 10^{-13}$	μ^-	$\mu_{rel.}^-$	t_{12}^+	$k_{CT}^+ \times 10^{-13}$	μ^+	$\mu_{rel.}^+$	μ^-/μ^+
I	0.037	9.42	2.65	1.00	0.066	29.2	8.21	1.00	0.32
II	0.023	3.22	0.77	0.29	0.085	48.5	11.55	1.41	0.07
III	0.015	1.77	0.42	0.16	0.039	10.5	2.49	0.30	0.17
IV	0.053	27.5	5.82	2.20	0.095	77.5	16.42	2.00	0.35
V	0.003	0.07	0.02	0.01	0.046	11.0	2.63	0.32	0.01
VI	0.015	1.99	0.47	0.18	0.011	0.52	0.12	0.02	3.85
VII [a]	0.034	6.88	2.25	1.18	—	—	—	—	—
VIII [b]	0.01	0.46	0.24	0.09	0.01	0.57	0.30	0.04	0.40

[a] from reference [23]. [b] from reference [33]

Charge injection properties. E_{LUCO} and E_{HOCO} (Energies of the LUCO and HOCO) calculated for oligomers of different chain lengths, as well as the corresponding energy values estimated for the infinite polymer chains, are shown Figure 8 ($r^2 \geq 0.998$ was obtained in all fits, see Tables 12S – 14S in Supplementary Information). For charge injection, a good ohmic contact is generally expected when $|\Phi - E_{LUCO/HOCO}| < 0.3$ eV and, therefore, low/high E_{LUCO}/E_{HOCO} values should facilitate the electron injection into *n*-type/*p*-type semiconductors.[34] For electron injection, oligomers **IV**, **V** and **VI** with $n \geq 5$ could satisfy this condition with commonly used electrodes such as Ca (Φ = -2.9 eV), Mg (Φ = -3.7 eV), and Al (Φ = -4.3 eV).[42,57] The lowest E_{LUCO} values were estimated for polymer **IV**, while polymers **III**, **V** and **VI** showed analogous values. An E_{LUCO} value close to that reported for polymer **VII** (-3.148 ± 0.015 eV)[23] was estimated for polymer **I**. Nevertheless, a significantly higher E_{LUCO} value has been reported for the reference polymer without nitrogen atoms in its chemical formula (**VIII**) (-2.56 eV).[33] Regarding hole injection, different metal oxides such as WO_3 (Φ = -6.8 eV), MoO_3 (Φ = -6.8 eV), NiO (Φ = -6.3), CuO (Φ = -5.9 eV), MoO_2 (Φ = -5.9 eV) and MoO_3/Al (Φ = -5.49 eV)[101] must produce nearly ohmic hole-injection contact with the majority of the studied

PAEs.[102,103] Moreover, polymers with a narrow band gap between HOCO and LUCO energies are usually more suitable to be employed as ambipolar semiconductors with the same type of electrodes. In general, the calculated band gap for the set of studied PAEs is not narrow enough to clearly assert both ohmic electron- and hole-injection contact with the same electrode. Only for the polymers with narrowest band gap, i.e. polymers **IV** and **VI**, nearly ohmic metal/polymer contact for both holes and electrons could be expected (see Figure 8).

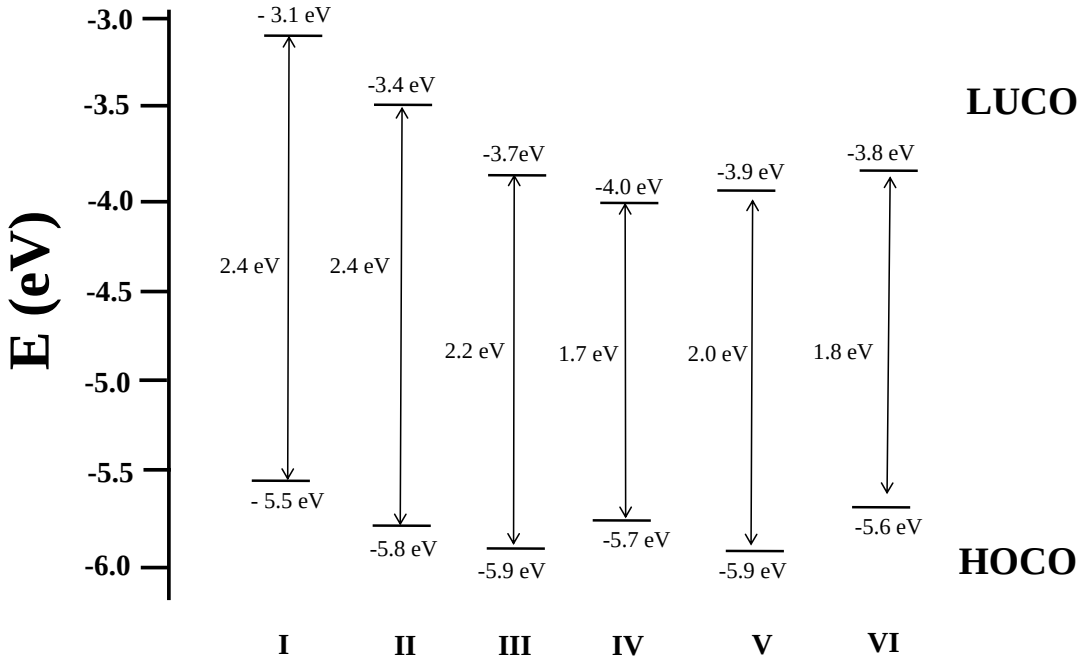

Figure 8. HOCO and LUCO energies estimated for the studied polymers.

The easines of charge injection can be complementarily analyzed through the values of EA and IP. Table 3 also shows the vertical and adiabatic EAs and IPs (VEA, AEA, VIP, and AIP) calculated for the infinite polymer chains (values calculated for the different oligomers are collected in Tables 8S and 9S, while the values from the different fits are showing in Tables 10S and 11S in the Supplementary Information). Thus, the AEAs estimated for the infinite polymer chains **II** – **VI** are within the range of 3.0 − 4.0

eV proposed by Newman *et al*.[42] for *n*-type organic semiconductors, hence the most favorable electron injection can be expected for polymer **I**. Likewise, IP must be low enough to allow an easy hole injection into the HOCO the semiconductor. In this sense, the lowest AIPs, along with the highest E_{HOMO} values, were obtained for polymer **I**, followed by polymers **IV** and **VI**. The lowest differences between AEA and AIP values, and consequently the narrowest band gaps, were estimated for polymers **IV** and **VI**, i.e. the only cases where ambipolar charge injection could be expected.

CONCLUSION

In the present work, the molecular structure and electronic properties of isolated chains, in addition to their polymer crystal structure of a set of PAEs containing TTh and arene diimide units linked by -C≡C- bridges have been systematically studied by means of DFT calculations. We can extract the following conclusions: i) all the polymer chains were found highly planar with structural stacking distance of 3.5 Å in all cases, except for polymers **I** (3.8 Å) and **IV** (3.3 Å); ii) the optical band gap decreases with the chain length and with the number of fused aromatic rings (for oligomers **I** – **IV**), exhibiting calculated band gaps for the oligomers **IV** with $n \geq 3$ (at the TD-B3LYP and TD-PBE0 levels) which satisfy one of the key requeriments for fabrication of solar cell devices made on organic semiconductors.

Regarding charge injection and transport, we can infer that: iii) the lowest λ_i^- values were estimated for the polymers with a larger number of fused rings in arene diimide unit, i.e. polymers **IV** (0.020 ± 0.004 eV) and **VI** (0.023 ± 0.004 eV), also observing how the presence of nitrogen atoms in TTh unit is a key factor to decrease λ_i^- values compared to reference oligomers **VII** and **VIII**. Moreover, λ_i^- values calculated for monomers **IV** – **VI** and for oligomers **I** – **III** with $n = 3$ are comparable or lower than

those calculated for some compounds proposed as *n*-type organic semiconductors; iv) in the case of hole transport, the lowest λ_i^+ was also estimated for polymer **IV** (0.024 ± 0.002 eV), obtaining the lower λ_i^+ values for oligomers with linkages to the core rather than those with linkages to the imide position. Those λ_i^+ values are comparable to those reported for some compounds with a demonstrated high mobility *p*-type semiconductors in electronic devices; v) The electronic coupling was calculated for dimers of stacked chains, taken from the previously modelled crystal structure. t_{12}^+ values are at least 1.8-fold higher than the corresponding t_{12}^- values except for polymer **VI**. The highest t_{12}^- and t_{12}^+ values were calculated for the polymer with the smallest stacking distance (**IV**) while low electronic couplings were in general obtained for those containing C-N linkages in the polymer backbone. We have also observed that the presence of nitrogen atoms in the electron-accepting unit seems to increase the t_{12}^- value in this kind of polymers as comparable t_{12}^- values were calculated and reported for polymers **I** and **VIII** and similar to polymer **VII**. Both highest t_{12}^- and t_{12}^+ values were calculated for polymer **IV**. In general, a more pronounced *p*-type rather than *n*-type character is expected for the studied PAEs since k_{CT}^+ / k_{CT}^- ratios are within 3 – 15 for polymers **I** – **IV**, being the highest absolute μ^+ and μ^- values obtained for polymer **IV**, which shows a relatively balanced μ^- / μ^+ ratio of 0.35 and could exhibit hopefully ambipolar behaviour.

Finally, for charge injection, the lowest E_{LUCO} and highest AEA were estimated for polymer **IV**, obtaining the highest E_{HOCO} and lowest AIP for polymer **I** (with similar values estimated for polymer **IV**), while the lowest differences between AEA and AIP values, and consequently the narrowest band gaps, were estimated for polymers **IV** and **VI**.

ACKNOWLEDGEMENTS

We gratefully acknowledge Supercomputing Service of Castilla-La Mancha University for allocation of computational resources. Mónica Moral Muñoz thanks to the E2TPCYTEMA-SANTANDER program for their financial support.

REFERENCES

[1] Arias, C.; MacKenzie, J. D.; McCulloch, I.; Rivnay, J.; Salleo, A. Materials and Applications for Large Area Electronics: Solution-Based Approaches. *Chem. Rev*., **2010**, *110*, 3–24.

[2] Guo, X.; Facchetti, A.; Marks, T. J. Imide- and Amide-Functionalized Polymer Semiconductos. *Chem. Rev.*, **2014**, *114*, 8943–9021.

[3] Brédas, J. L.; Beljonne, D.; Coropceanu, V.; Cornil, J. Charge-Transfer and Energy-Transfer Processes in π-Conjugated Oligomers and Polymers: A Molecular Pictures. *Chem. Rev*., **2004**, *104*, 4971–5004.

[4] Hutchison, G. R.; Ratner, M. A.; Marks, T. J. Intermolecular Charge Transfer between Heterocyclic Oligomers. Effects of Heteroatom and Molecular Packing on Hopping Transport in Organic Semiconductors. *J. Am. Chem. Soc*., **2005**, *127*, 16866–16881.

[5] Yasuda, T.; Imase, T.; Sasaki, S.; Yamamoto, T. Synthesis, Solid Structure, and Optical Properties of New Thiophene-Based Alternting π-Conjugated Copolymers Containing 4-Alkyl-1,2,4-triazole or 1,3,4-Thiadiazole Unit as Partner Unit. *Macromolecules*. **2005**, *38*, 1500–1503.

[6] Yasuda, T.; Imase, T.; Nakamura, Y.; Yamamoto, T. New Alternative Donor−Acceptor Arranged Poly(Aryleneethynylene)s and Their Related Compounds Composed of Five-Membered Electron-Accepting 1,3,4-Thiadiazole, 1,2,4-Triazole,

or 3,4-Dinitrothiophene Units: Synthesis, Packing Structure, and Optical Properties. *Macromolecules*. **2005**, *38*, 4687–4697.

[7] Jansson, E.; Jha, P. C.; Ågren, H. Density Functional Study of Triazole and Thiadiazole Systems as Electron Transporting Materials. *Chem. Phys*., **2006**, *330*, 166–171.

[8] Sato, M.; Tada, Y.; Nakashima, S.; Ishikura, K. I.; Handa, M.; Kasuga, K. Synthesis and Optical and Electrochemical Properties of Thermotropic, Liquid-crystalline, Semirigid Copolyesters Based on 2,3-Diphenyl-1,3,4-Thiadiazole Units. *J. Polym. Sci., Part A: Polymer Chemistry*, **2005**, *43*, 1511–1525.

[9] Bunz, U. H. F. Poly(aryleneethynylene)s: Syntheses, Properties, Strucctures, and Applications. *Chem. Rev.*, **2000**, *100*, 1605–1644.

[10] Cimrová, V.; Ulbricht, C.; Dzhabarov, V.; Výprachtický, D.; Mbi Egbe, D. A. New Electroluminiscent Carbazole-Containing Conjugated Polymer: Synthesis, Photophysics, and Electroluminiscence. *Polymer*, **2014**, *55*, 6220–6226.

[11] Kim, J.; Han, A. R.; Hong, J.; Kim, G.; Lee, J.; Joo Shin, T.; Hak Oh, J.; Yang. C. Ambipolar Semiconducting Polymer π-Spacer Linked Bsi-Benzothiadiazole Blocks as Strong Accepting Units. *Chem. Mater*. **2014**, *26*, 4933–4942.

[12] Shi, W.; Wang, L.; Umar, M.; Awut, T.; Mi, H.; Tan, C.; Nurulla, I. Novel Poly(arylene ethynylene) Derivatives Containing Main Chain Triphenylamine and Pendent Quinoxaline Moieties: Synthesis and Elementary Characterization. *Polym. Int.*, **2009**, *58*, 800–806.

[13] Weder, C. *Poly(aryleneethynylene)s: From Synthesis to Application* (Advances in Polymer Science). Springer. Heidelberg, **2005**.

[14] Wei, J.; Zhang, X.; Zhao, Y.; Li, R. Chiral Conjugated Microporous Polymers as Novel Chiral Fluorescence Sensor for Amino Alcohols. *Macromol. Chem. Phys*., **2013**, *214*, 2232–2238.

[15] Beeby, A.; Findlay, K. S.; Low, F. J.; Marder, T. B.; Matousek, P.; Parker, A. W.; Rutter, S. R.; Towrie, M. Studies of S_1 State in a Prototypical Molecular Wire Using Picosecond Time-Resolved Spectroscopies. *Chem. Commun*., **2003**, 2406–2407.

[16] Beeby, A.; Findlay, K. S.; Low, F. J.; Marder, T. B. A Re-Evaluation of Photophysical Properties of 1,4-Bis(phenylethynyl)benzene: A Model for Poly(Phenyleneethynylene). *J. Am. Chem. Soc*., **2002**, *124*, 8280–8284.

[17] Greaves, S. J.; Flynn, E. L.; Futcher, F. L.; Wrede, E.; Lydon, D. P.; Low, P. J.; Rutter, S. R.; Beeby, A. Cavity Ring-Down Spectroscopy of The Torsional Motions of 1,4-Bis(phenylethynyl)benzene. *J. Phys. Chem. A*. **2006**, *110*, 2114–2121.

[18] Levitus, M.; Schmieder, K.; Ricks, H.; Shimizu, K. D.; Bunz, U. H. F.; García-Garabay, M. A. Steps to Demarcate the Effects of Chromophore Aggregation and Planarization in Poly(PHenyleneethynylene)s. 1. Rotationally Interrupted Conjugation in the Excited States of 1,4-Bis(phenylethynyl)benzene. *J. Am. Chem. Soc*., **2001**, *123*, 4259–4265.

[19] Granadino-Roldán, J. M.; Garzón, A.; García, G.; Peña-Ruiz, T.; Fernández–Liencres, M. P.; Navarro, A.; Fernández-Gómez, M. Theoretical Study of the Effect of Ethynyl Group on the Structure and Electrical Properties of Phenyl-Thiadiazole Systems as Precursors of Electron-Conducting Materials. *J. Chem. Phys*. **2009**, *130*, 234907-1–234907-10.

[20] Garzón, A.; Granadino-Roldán, J. M.; Moral, M.; García, G.; Fernández-Liencres, M. P.; Navarro, A.; Peña-Ruiz, T.; Fernández-Gómez. M. Density Funcitonal Theory Study of the Optical and Electronic Properties of Oligomers Base don Phenyl-Ethynyl

Units Linked to Triazole, Thiadiazole, and Oxadiazole Rings to Be Used in Moleuclar electronics. *J. Chem. Phys*., **2010**, *132*, 064901-1–064901-11.

[21] Granadino-Roldán, J. M.; Garzón, A.; García, G.; Moral, M.; Navarro, A.; Fernández-Liencres, M. P.; Peña-Ruiz, T.; Fernández-Gómez, M. Theoretical Study of the Effect of Alkyl and Alkoxy Lateral Chains on the Structural and Electronic Properties of π-Conjugated Polymers Consisting of Phenylethynyl-1,3,4-Thiadiazole. *J. Phys. Chem. C*., **2011**, *115*, 2865–2873.

[22] Garzón, A.; Granadino-Roldán, J. M.; García, G.; Moral, M.; Fernández-Gómez, M. Crystal Structure and Charge Transport Properties of Poly(arylene-ethynylene) Derivatives: A DFT Approach. *J. Chem. Phys*. **2013**, *138*, 154902-1–154902-6.

[23] Moral, M.; García, G.; Garzón, A.; Granadino-Roldán, J. M.; Fernández-Gómez, M. DFT Study of the Effect of Fluoringe Atoms on the Crystal Structure and Semiconducting Properties of Poly(arylene-ethylene) derivatives. *J. Chem. Phys.*, **2016**, *144*, 154902-1–154902-10.

[24] Osaka, I.; Zhang, R.; Sauvé, G.; Smilgies, D. M.; Kowalewski, T.; McCullough, R. D. High-Lamellar Orderin and Amorphous-Like π-Network in Short-Chain Thiazolothiazole-Thiophene Copolymers Lead to High Mobilities. *J. Am. Chem. Soc*. **2009**, *131*, 2521–2529.

[25] Wudl, N.; Wudl, F. Two Poly(2,5-Thienylthiazolothiazole)s: Observation of Spontaneous Ordering in Thin Films. *Macromolecules*. **2008**, *41*, 3169–3174.

[26] Ando, S.; Kumaki, D.; Nishida, J.; Tada, H.; Inoue, Y.; Tokito, S.; Yamashita, Y. Synthesis, Physical Properties and Field-Effect Transistors of Novel Thiazolothiazole-Penhylene Co-oligomers. *J. Mater. Chem.*, **2007**, *17*, 553–558.

[27] Ando, S.; Nishida, J.; Fujiwara, E.; Tada, H.; Inoue, Y.; Tokito, S.; Yamashita, Y. Physical Properties and Field-Effect Transistors Base don Novel

Thiazolothiazole/Heterocyclic and Thiazolothiazole/Phenylene Co-Oligomres. *Synth. Metals*, **2006**, *156*, 327–331.

[28] Shi, Q.; Fan, H.; Liu, Y.; Chen, J.; Shuai, Z.; Hu, W.; Li, Y.; Zha, X. Thiazolothiazole-Containing Polythiophenes with Low HOMO Level and High Hole Mobility for Polymer Solar Cells. *J. Polymer. Sci. A: Polymer. Chem*., **2011**, *49*, 4875–4885.

[29] Sanyal, S.; Manna, A. K.; Pati, S. K. Effect of Imide Functionalization on the Electronic, Optical, and Charge Transport Properties of Coronene: A Theoretical Study. *J. Phys. Chem. C.*, **2013**, *117*, 825–836.

[30] Hariharan, M.; Siegmund, K.; Zheng, Y.; Long, H.; Schatz, G. C.; Lewis, F. D. Perylenediimide-Linked DNA Dumbbells: Long-Distance Electronic Interactions and Hydrophobic Assitance of Base-Pair Melting. *J. Phys. Chem. C*, **2010**, *114*, 20466–20471.

[31] Grazulevicius, J. V.; Strohriegl, P.; Pielichowski, J.; Pielichowski, K. Carbazole-Containing Polymers: Synthesys, Properties and Applications. *Prog. Polym. Sci.*, 2003, 28, 1297–1353.

[32] García, G.; Garzón, A.; Granadino-Roldán, J. M.; Moral, M.; Navarro, A.; Fernández-Gómez, M. Optoelectronic and Charge Transport Properties of Oligomers Based on Phenylethynylene Units Linked to Thieno-acenes: A DFT Study. *J. Phys. Chem. C*, **2011**, *115*, 6922–6392.

[33] García, G.; Moral, M.; Garzón, A.; Granadino-Roldán, J. M.; Navarro, A.; Fernández-Gómez, M. Poly(arylenethynyl-thienoacenes) as Candidate for Organic Semiconducting Materials. A DFT Insight. *Org. Elect*., **2012**, *13*, 3244–3253.

[34] Wang, L.; Nan, G.; Yang, X.; Peng, Q.; Li, Q.; Shuai, Z. Computational Methods for Desing of Organic Materials with High Charge Mobility. *Chem. Soc. Rev*., **2010,** *39*, 423–434.

[35] Chen, X-K.; Zou, L-Y.; Min, C-G.; Ren, A-M.; Feng, J-K.; Sun, C-C. Theoretical Investigation of Charge Injection and Transport Properties of Novel Organic Semiconductor Materials-Cyclic Oligothiophenes. *Org. Electron.*, **2011**, *12*, 1198–1210.

[36] Duhm, S.; Xin, Q.; Hosoumi, S.; Fukagawa, H.; Sato, K.; Ueno, N.; Kera, S. Charge Reorganization Energy and Small Polaron Binding Energy of Rubrene Thin Films by Ultraviolet Photoelectron Spectroscopy. *Adv. Mater.*, **2012**, *24*, 901–905.

[37] Marcus, R. A. Electron Transfer Reactions in Chemistry. Theory and Experiment. *Rev. Mod. Phys*., **1993**, *65*, 599.

[38] Barbara, P. F.; Meyer, T. J.; Ratner, M. A. Contemporary Issues in Electron Transfer Research. *J. Phys. Chem*., **1996**, *100*, 13148–13168.

[39] Stehr, V.; Fink, R. F.; Tafipolski, M.; Deibel, C.; Engels, B. Comparison of Different Rate Constant Expressions for the Prediction of Charge and Energy Transport in Oligoacenes. *WIREs Comput. Mol. Sci.*, **2016**, doi: 10.1002/wcms.1273.

[40] Olivier, Y.; Lemaur, V.; Brédas, J. L.; Cornil, J. Charge Hopping in Organic Semiconductors: Influence of Molecular Parameters on Macroscopic Mobilities in Model One-Dimensional Stacks. *J. Phys. Chem. A* **2006**, *110*, 6356–6364

[41] Burquel, A.; Lemaur, V.; Beljonne, D.; Lazzaroni, R.; Cornil, J. Pathways for Photoinduced Charge Separation and Recombination at Donor-Acceptor Heterojunctions: The Case of Oligophenylenevinylene-Perylene Bisimide Complexes. *J. Phys. Chem. A* **2006**, *110*, 3447–3453

[42] Newman, C. R.; Frisbie, C. D.; da Silva Filho, D. A.; Brédas, J. L.; Ewbank, P. C.; Mann, R. K. Introduction to Organic Thin Film Transistors and Desing of n-Channel Organic Electronic. *Chem. Mater*. **2004**, *16*, 4436–4451.

[43] Troisi, A. Charge Transport in High Mobility Molecular Semiconductors: Classical Models and New Theories. *Chem. Soc. Rev*., **2011**, *40*, 2347–2358.

[44] Coropceanu, V.; André, J. M.; Malagoli, M.; Brédas, J. L. The Role of Vibronic Interactions on Intramolecular and Intermolecular Electron Transfer in π-Conjugated Oligomers. *Theor. Chem. Acc*., **2003**, *110*, 59–69.

[45] Coropceanu, V.; Cornil, J.; da Silva Filho, D. A.; Olivier, Y.; Silbey, R.; Brédas, J. L. Charge Transport in Organic Semiconductors. *Chem. Rev*., **2007**, *107*, 926–952.

[46] McMahon, D. P.; Troisi, A. Evaluation of the External Reorganization Energy of Polyacenes. *J. Phys. Chem. Lett*., **2010**, *1*, 941–946.

[47] Norton, J.E.; Brédas, J. L. Polarization Energies in Oligoacene Semiconductor Crystals. *J. Am. Chem. Soc*. **2008**, *130*, 12377–12384.

[48] Martinelli, N. G.; Savini, M.; Muccioli, L.; Olivier, Y.; Castet, F.; Zannoni, C.; Beljonne, D.; Cornil, J. Modeling Polymer Dielectric/Pentacene Interfaces: On the Role of Electrostatic Energy Disorder on Charge Carrier Mobility. *Adv. Funct. Mater*., **2009**, *19*, 3254–3261.

[49] Lemaur, V.; Steel, M.; Beljonne, D.; Brédas, J. L.; Cornil, J. Photoinduced Charge Generation and Recombination Dynamics in Model Donor/Acceptor Pairs for Organic Solar Cell Applications: A Full Quantum-Chemical Treatment. *J. Am. Chem. Soc*. **2005**, *127*, 6077–6086.

[50] Nelsen, S. F.; Yunta, M. J. R. Estimation of Marcus λ for p-Phenylenediamines from the Optical Spectrum of a Dimeric Derivative. *J. Phys. Org. Chem*. **1994**, *7*, 55–62.

[51] Nelsen, S. F.; Blackstock, S. C.; Kim, Y. Estimation of Inner Shell Marcus Therms for Amino Nitrogen Compounds by Molecular Orbital Calculations. *J. Am. Chem. Soc*. **1987**, *109*, 677–682.

[52] Cheung, D. L.; Troisi, A. Modelling Charge Transport in Organic Semiconductors: From Quantum Dynamics to Soft Matter. *Phys. Chem. Chem. Phys*., 2008, 10, 5941–5952.

[53] Sancho-García, J. C. Application of Double-Hybrid Density Functional of Charge Transfer in N-substituted Pentacenequinones. *J. Chem. Phys*., **2012**, *136*, 174703.

[54] Kera, S.; Yamane, H.; Ueno, N. First-principles Measurements of Charge Mobility in Organic-Semiconductors: Valence Hole-Vibration Coupling in Organic Ultrathin Films. *Proc. Surf. Science*., **2009**, *54*, 135–154.

[55] Yavuz, I.; Martin, B. N.; Park, J.; Houk, K. N. Theoretical Study of the Molecular Ordering, Paracrystallinity, And Charge Mobilities of Oligomers in Different Crystalline Phases. *J. Am. Chem. Soc.* **2015**, *137*, 2856−2866

[56] Sun, S. S.; Dalton, L. R. Introduction to Organic Electronic and Optoelectronic Materials and Devices; CRC Press: Taylor & Francis Group, New York, **2005**.

[57] Michaelson, H. B. The Work Function of the Elements and its Periodicity. *J. Appl. Phys*., **1977**, *48*, 4729–4733.

[58] Körzdörfer, T.; Parrish, R. M.; Sears, J. S.; Sherrill, C. D.; Brédas, J. L. On the Relationship between Bond-Length Aleternation and Many-Electron Self-Interaction Error. *J. Chem. Phys.*, **2012**, *137*, 124305.

[59] Anthopoulos, T. D.; Anyfantis, G. C.; Papavassiliou, G. C.; de Leeuw, D. M. Air-Stable Ambipolar Organic Transistors. *Appl. Phys. Lett.*, **2007**, *90*, 122105.

[60] Zhan, X.; Facchetti, A.; Barlow, S.; Marks, T. J.; Ratner, M. A.; Wasielewski, M. R.; Marder, S. R. Rylene and Related Diiides for Organic Electronics. *Adv. Mater*., **2011**, *23*, 268–284.

[61] Frisch, M. J.; Trucks, G. W.; Schlegel, H. B.; Scuseria, G. E.; Robb, M. A.; Cheeseman, J. R.; Scalmani, G.; Barone, V.; Mennucci, B.; Petersson, G.A.; *et al*. Gaussian 09, revision D.01; Gaussian Inc.: Wallingford, CT, **2009**.

[62] Becke, A. D. Density-Functional Termochemistry. III. The Role of Exact Exchange. *J. Chem. Phys*. **1993**, *98*, 5648–5652.

[63] Lee, C.; Yang, W.; Parr, R. G. Development of the Coll-Salvetti Correlation-Energy Formula into a Functional of the Electron Density. *Phys. Rev. B*. **1988**, *37*, 785–789.

[64] Perdew, J. P.; Burke, K.; Ernzerhof, M. Generalized Gradient Approximation Made Simple. *Phys. Rev. Lett*., **1996**, *77*, 3865.

[65] Zhao, Y.; Truhlar, D. G. The M06 Suite of Density Funcitonal for Main Group Thermochemistry, Thermochemical Kinetics, NonCovalent Interactions, Excited States, and Transition Elements: Two New Functional and Systematic Testin of Four M06-class Functional and 12 other Functionals. *Theor. Chem. Acc*., **2008**, *120*, 215–241.

[66] Jacquemin, D.; Perpète, E. A.; Coifini, I.; Adamo, C. Accurate Simulation of Optical Properties in Dyes. *Acc. Chem. Res*., **2009**, *42*, 326–324.

[67] Moral, M.; García, G.; Peñas, A.; Garzón, A.; Granadino-Roldán, J. M.; Melguizo, M.; Fernández-Gómez, M. Eletronic Properties of Diphenyl-*s*-tetrazine and Some Related Oliogomers. An Spectroscopy and Theoretical Chemistry. *Chem. Phys*., **2012**, *408*, 17–27.

[68] Moral, M.; Garzón, A.; García, G.; Granadino-Roldán, J. M.; Fernández-Gómez, M. DFT Study of the Ambipolar Character of Polymers on the Basis of *s*-Tetrazine and Aryl Rings. *J. Phys. Chem. C*. **2015**, *119*, 4588–4599.

[69] Granadino-Roldan, J. M.; Garzón, A.; Moral, M.; García, G.; Peña-Ruiz, T.; Fernández-Liencres, M. P.; Navarro, A.; Fernández-Gómez, M. Theoretical EStimation of the Optical Bandgap in a Series of Poly(aryl-ethynylene)s: A DFT Study. *J. Chem. Phys*., **2014**, *140*, 044908-1–044908-5.

[70] Meier, H.; Stalmach, U.; Kolshorn, H. Effective Conjugation Length and UV/vis Spectra of Oligomers. *Acta Polym*., **1997**, *48*, 379–384.

[71] García, G.; Granadino-Roldán, J. M.; Garzón, A.; Moral, M.; Peña-Ruiz, T.; Navarro, A.; Fernández-Liencres, M. P.; Fernández-Gómez, M. Theoretical Study of Bis(Phenylethynyl)thienoacenes as Precursor of Molecular Wires for Molecular Electronics. *J. Phys. Chem. C*., **2010**, *114*, 12325–12334.

[72] Hung, Y. C.; Jiang, J. C.; Chao, C. Y.; Su, W. F.; Lin, S. T. Theoretical Study on the Correlation between Band Gap, Bandwidth, and Oscillator Strenght in Fluorene-Based Donor-Acceptor Conjugated Copolymers. *J. Phys. Chem. B.*, **2009**, *113*, 8268–8277.

[73] Lin, B. C.; Cheng, C. P.; Lao, Z. P. M. Reorganization Energy in the Transports of Holes and Electrons in Organic Amines in Organic Electroluminiscence Studied by Density Functional Theory. *J. Phys. Chem. A*, **2003**, *107*, 5241–5251.

[74] Randic, M. Aromaticity of Polycyclic Conjugated Hydrocarbons. *Chem. Rev.*, **2003**, *103*, 3449–3606.

[75] Coropceanu, V.; Malagoli, M.; da Silva Filho, D. A.; Gruhn, N. E.; Bill, T. G.; Brédas, J. L. Hole- and Electron-Vibrational Coupling in Oligoacene Crystals: Intramoleuclar Contributions. *Phys. Rev. Lett*., **2002**, *89*, 275503−275507.

[76] Zhan, C. G.; Nichols, J. A.; Dixon, D. A. Ionization Potential, Electron Affinity, Electronegativity, Hardness, and Electron Excitation Energy: Molecular Properties from Density Functional Theory. *J. Phys. Chem. A.*, **2003**, *107*, 4184–4195.

[77] Rienstra-Kiracofe, J. C.; Tschumper, G. S.; Schaefer III, H. F.; Nandi, S.; Ellison, G. B. Atomic and Molecular Electron Affinities: Photoelectron Experiments and Theoretical Computations. *Chem. Rev.*, **2002**, *102*, 231–282.

[78] Rienstra-Kiracofe, J. C.; Barden, C. J.; Brown, S. T.; Schaefer III, H. F. Electron Affinites of Polycyclic Aromatic Hydrocarbons. *J. Phys. Chem. A.*, **2001**, *105*, 524–528.

[79] Muscat, J.; Wander, A.; Harrison, N. M. On the Prediction of Band Gaps from Hybrid Functional Theory. *Chem. Phys. Lett.*, **2001**, *342*, 397–401.

[80] Tsuneda, T.; Song, J. W.; Suzuki, S.; Hirao, J. On Koopmans' Theorem in Density Functional Theory. *J. Chem. Phys.*, **2010**, *133*, 174101.

[81] Heyd, J.; Scuseria, G. E. Efficient Hybrid Density Functional Calculations in Solids: Assessment of the Heyd-Scuseria-Ernzerhof Screened Coulomb Hybrid Functional. *J. Chem. Phys.*, **2004**, *121*, 1187.

[82] Heyd, J.; Peralta, J. E.; Scuseria, G. E.; Martin, R. L. Energy Band Gaps and Lattice Parameters Evaluated with the Heyd-Scuseria-Ernzerhof Screened Hybrid Functional. *J. Chem. Phys*., **2005**, *123*, 174101.

[83] Krukau, A. V.; Vydrov, A. O.; Izmaylov, A. F.; Scuseria, G. E. Influence of the Exchange Screening Parameter of the Performance of Screened Hybrid Functionals. *J. Chem. Phys*., **2006**, *125*, 224106.

[84] Mühlbacher, D.; Scharber, M.; Morana, M.; Zhu, Z.; Waller, D.; Gaudiana, R.; Brabec, C. High Photovoltaic Performances of a Low-Bandgap Polymer. *Adv. Mater*., **2006**, *18*, 2884–2889.

[85] Guo, X.; Watson, M. D. Pyromellitic Diimide-Based Donor-Acceptor Poly(phenyleneethynylene)s. *Macromolecules*, **2011**, *44*, 6711–6716.

[86] Jones, B. A.; Facchetti, A.; Wasielewski, M. R.; Marks, T. J. Tuning Orbital Energetics in Arylene Diimide Semiconductors. Materials Design for Ambient Stability of n-Type Charge Transport. *J. Am. Chem. Soc.*, **2007**, *129*, 15259–15278.

[87] Li, D.; Zhang, Z.; Zhao, S.; Wang, Y.; Zhang, H. Diboron-Containing Fluorophores with Extended Ladder-type π-Conjugated skeletons. *Dalton Trans*., **2011**, *40*, 1279–1285.

[88] Olgun, U.; Gülfen, M. Synthesis of Fluorescence Poly(Phenylenethiazolo[5,4-d]thiazole) Copolymer Dye: Spectroscopy, Cyclic Voltammetry and Thermal Analysis. *Dyes and Pigments*, **2014**,*102*, 189–195.

[89] Lin, B. C.; Cheng, C. P.; You, Z. Q.; Hsu, C. P. Charge Transport Properties of Tris (8-hydroxyquinolinato)aluminum (III): Why It Is an Electron Transport. *J. Am. Chem. Soc*., **2005**, *127*, 66–67.

[90] Rawson, J.; Angiolillo, P. J.; Therien, M. J. Extreme Electron Polaron Spatial Delocalization in π-Conjugated Materials. *PNAS*., **2015**, *112*, 13779–13783.

[91] Chesterfield, R. J.; McKeen, J. C.; Newman, C. R.; Ewbank, P. C.; da Silva Filho, D. A.; Brédas, J. L.; Miller, L. L.; Mann, K. R.; Frisbie, C. D. Organic Thin Film Transistors Based on N-Alkyl Perylene Diimides: Charge Transport Kinetics as a Function of Gate Voltage and Temperature. *J. Phys. Chem. B*., **2004**, *108*, 19281–19292.

[92] McGarry, K. A.; Xie, W.; Sutton, C.; Risko, C.; Wu, Y.; Young, W. G.; Brédas, J. L.; Frisbie, C. D.; Douglas, C. J. Rubrene-Based Single Crystal Organic Semiconductors: Synthesis, Electronic Structure, and Charge-Transport Properties. *Chem. Mater.*, **2013**, *25*, 2254–2263.

[93] Fazzi, D.; Castiglioni, M. C. C. Quantum-Chemical Insigths into the Prediction of Charge Transport Parameters for a Napthalenetetracarboxydiimide-Based Copolylmers With Enhanced Electron Mobility. *J Am Chem Soc*., **2011**, *133*, 19056–19059.

[94] Xiao, J; Liu, X-K.; Wang, X-X.; Zheng, C-J.; Li, F. Tailoring Electronic Structure of Organic Host for High-Performance Phosphorescent Organic Light-Emitting Diodes. *Org. Electron.*, **2014**, *15*, 2763–2768.

[95] Otón, F.; Pfattner, R.; Pavlica, E.; Olivier, Y.; Moreno, E.; Puigdollers, J.; Bratina, G.; Cornil, J.; Fontrodona, X.; Mas-Torrent, M.; *et al.* Electron-Withdrawing Substituted Tetrahiafulvalenes as Ambipolar Semiconductors. *Chem. Mater*., **2011**, *23*, 851–861.

[96] Sokolov, A. N.; Atahan-Evrenk, S.; Mondal, R.; Akkerman, H. B.; Sánchez-Carrera, R. S.; Granados-Focil, S.; Schrier, J.; Mannsfeld, S. C. B.; Zoombelt, A. P.; Bao, Z.; Aspuru-Guzik, A. From Computational Discovery to Experimental Characterization of a High Hole Mobility Organic Crystal. *Nature Commun*., **2011**, *437*, 1–8.

[97] Sánchez-Carrera, R. S.; Paramonov, P.; Day, G. M.; Coropceanu, V.; Brédas, J. L. Interaction of Charge Carriers with Lattice Vibrations in Oligoacene Crystals from Naphthalene to Pentacene. *J. Am. Chem. Soc*., **2010**, *132*, 14437–14446.

[98] Koh, S. E.; Risko, C.; da Silva Filho, D. A.; Kwon, O.; Facchetti, A.; Brédas, J. L.; Marks, T. J.; Ratner, M. A. Modelling Electron and Hole Transport in Fluoroacene-Oligothiophene Semiconductors: Investigacion of Geometric and Electronic Structure Properties. *Adv. Funct. Mater*., **2008**, *18*, 332–340.

[99] Sahu, H.; Panda, A. N. Computational Investigation of Charge Injection and Transport Properties of a Series of Thiophene-Pyrrole Based Oligo-Azomethines. *Phys. Chem. Chem. Phys*. **2014**, *16*, 8563–8574.

[100] Kojima, H.; Mori, T. Estimated Mobility of Ambipolar Organic Semiconductors, Indigo and Diketopyrrolopyrrole. *Chem. Lett*., **2013**, *42*, 68–70.

[101] Xue, Z.; Liu, X.; Lv, Y.; Zhang, N.; Guo, X. Low-Work-Function, ITO-Free Transparent Cathodes for Inverted Polymer Solar Cells. *Appl. Mater. Interfaces*, **2015**, *7*, 19960 – 19965.

[102] Greiner, M. T.; Chai, L.; Helander, M. G.; Tang, W. M.; Lu, Z-H. Transition Metal Oxide Work Functions: The Influence of Cation Oxidation State and Oxygen Vacancies. *Adv. Funct. Mater.*, **2012**, *22*, 4557–4568.

[103] Greiner, M. T.; Lu, Z.-H. Thin-Film Metal Oxides in Organic Semiconductor Devices: Their Electronic Structures, Work Functions and Interfaces. *NPG Asia Mater.*, **2013**, *5*, 1−16.